

Estimating Uncertainty of Autonomous Vehicle Systems with Generalized Polynomial Chaos

Keyur Joshi, Chiao Hsieh, Sayan Mitra, and Sasa Misailovic

University of Illinois Urbana-Champaign

Abstract. Modern autonomous vehicle systems use complex perception and control components and must cope with uncertain data received from sensors. To estimate the probability that such vehicles remain in a safe state, developers often resort to time-consuming simulation methods.

This paper presents an alternative methodology for analyzing autonomy pipelines in vehicular systems, based on Generalized Polynomial Chaos (GPC). We also present GAS, the first algorithm for creating and using GPC models of complex vehicle systems. GAS replaces complex perception components with a perception model to reduce complexity. Then, it constructs the GPC model and uses it for estimating state distribution and/or probability of entering an unsafe state.

We evaluate GAS on five scenarios used in crop management vehicles, self driving cars, and aerial drones – each system uses at least one complex perception or control component. We show that GAS calculates state distributions that closely match those produced by Monte Carlo Simulation, while also providing 2.3x-3.0x speedups.

1 Introduction

Autonomous vehicles are increasingly pervasive. They navigate by perceiving the vehicle’s state, making a control decision based on this *perceived* state, and moving accordingly. To ensure safety of life and property, their developers must ensure that the vehicle does not enter an unsafe state, which corresponds to undesirable outcomes such as crashes, immobilization, and moving off course. However, 1) many sensors give uncertain readings (e.g., GPS and LIDAR) and 2) the vehicle’s software processes sensor values or makes decisions using complex, possibly imperfect components such as neural networks and lookup tables. Due to this uncertainty, proving that an autonomous vehicle will *never* enter an unsafe state is impossible or impractical. Researchers instead focus on ensuring that an autonomous system will not enter an unsafe state *with high probability*, and use probabilistic and statistical techniques for system analysis.

Monte Carlo Simulation (MCS) is perhaps the most used general method for estimating the probability of entering an unsafe state over time. Unfortunately, MCS requires a large number of simulations (which may be too expensive to run) in order to get a sufficiently accurate estimate of the state distribution [21,27].

Analytical techniques for nonlinear dynamics and *uncertainty quantification* (UQ) are an attractive alternative to MCS for estimating the state distribution over time. *Generalized Polynomial Chaos* (GPC) is a well-known analytical

technique that has found many applications in physics and engineering [31]. GPC constructs a polynomial model of the simulated system (typically represented as a system of partial differential equations), using a limited number of system evaluations. Researchers then use the GPC model instead of the original system simulation to estimate the state distribution over time.

A complete autonomous vehicle system contains complex perception and control components alongside vehicle dynamics. While vehicle dynamics in isolation can be represented as differential equations [16], the same is not true for such complex perception and control components. Additionally, small input perturbations may significantly change their output. As a result, we cannot directly apply GPC for estimating the vehicle’s state distribution over time.

Our work. We present GAS (**GPC** for **A**utonomous **V**ehicle **S**ystems), the first approach for using GPC to analyze the navigation software pipeline of an autonomous vehicle system.

GAS first creates a *perception model* to represent the error of the perception system and overcome its sensitivity to inputs. GAS uses the perception model to estimate the output distribution of the state perception system. GAS then automatically constructs a GPC model of the perception model coupled with the remaining stages of the navigation system, and uses it to estimate the vehicle state distribution and statistical safety properties. We show that the outputs of GAS converge in distribution to the outputs of the original navigation system.

We use GAS to estimate the state distribution of vehicle systems over time in five scenarios. These scenarios model systems used in crop management vehicles, self driving cars, and aerial drones. Each vehicle system uses at least one complex perception or control component. We show that GAS produces state distribution estimates that closely match those calculated via MCS, while being 2.3x-3.0x faster. We also use GAS for global sensitivity analysis of the vehicle systems to initial state perturbations by calculating Sobol sensitivity indices [29].

Contributions. This paper makes several contributions:

- **State distribution estimation for complex autonomous vehicle systems.** We present GAS, a novel methodology and an algorithm for estimating the state distribution and statistical safety properties of complex autonomous vehicle systems over time using GPC.
- **Perception models for GPC.** We present models for complex perception systems that estimate the output distribution of the original systems. We use these perception models as part of our GAS approach.
- **Implementation.** We implement GAS as a tool which automates the creation of the perception model and the creation and usage of the GPC model.
- **Evaluation.** We evaluate GAS on five scenarios from self driving cars, aerial drones, and crop monitoring vehicles. GAS provides fast and accurate estimates of the vehicle state distribution over time and the global sensitivity of the vehicle systems.



Fig. 1: Real-life corn monitoring vehicle Fig. 2: Gazebo simulation overhead view Fig. 3: Gazebo simulation front camera view

2 Example

Consider a scenario from precision agriculture. An autonomous vehicle travels between two rows of corn in order to monitor crop growth and detect weeds. Farmers or other autonomous vehicles can use this information to adjust fertilizer and herbicide levels on a location to location basis. We have adapted this scenario from [28]. Figures 1-3 illustrate the scenario. The desired path is shown in red.

The top half of Figure 4 shows a block diagram representation of the system responsible for driving the vehicle between two rows of corn. First, a camera captures the area in front of the vehicle. The image depends on the current vehicle state as well as environmental conditions. The neural network analyzes the image to perceive the current vehicle state. The relevant state variables in this scenario are: 1) The *heading* angle h , which is the angle between the vehicle’s current heading and the imaginary centerline between the two rows of corn; h can take values in $[-\pi, \pi]$ radians, with 0 corresponding to the direction of the centerline. 2) The *distance* d of the vehicle from the centerline; d can take values in $[-0.38, 0.38]$ meters, with 0 corresponding to the centerline.

As neural networks are inherently approximate, the state perceived by the neural network may not be the same as the ground truth. The vehicle uses this approximate heading and distance reading to calculate a steering angle in order to keep the vehicle on the centerline. Finally, the vehicle moves according to its constant speed and commanded steering angle.

Unsafe States. We wish to avoid two undesirable outcomes: 1) if $|d| > 0.228m$, the vehicle will hit the corn, and 2) if $|h| > \pi/6$, the neural network output becomes highly inaccurate and recovery may be impossible. To avoid these outcomes, we want the vehicle to remain in the *safe region*, defined as all states with $d \in [-0.228, 0.228] \wedge h \in [-\pi/6, \pi/6]$. Because the vehicle makes steering decisions based on approximate data, we cannot be certain that the vehicle will remain safe. Instead, we answer the question: *What is the probability that the vehicle will remain safe over a period of time?*

Monte Carlo Simulation. In *Monte Carlo Simulation* (MCS), we simulate the vehicle’s movement a large number of times and count the number of times the vehicle reaches an unsafe state. We use Gazebo (Figures 2 and 3) for precise control over the simulation environment.

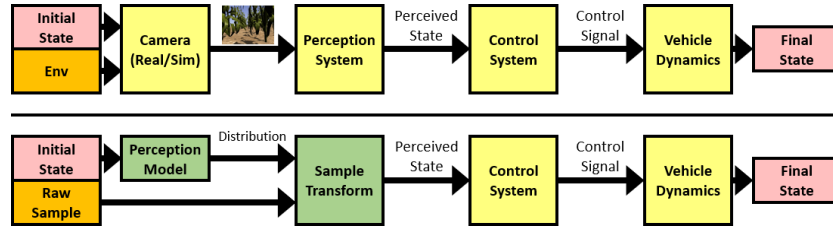


Fig. 4: Corn monitor vehicle model: original (top) and abstract (bottom)

We simulate 1000 samples over 100 time steps of 0.1 seconds each. We randomly sample environmental conditions and choose the initial vehicle state from a normal distribution. For each sample at each time step, we invoke the *vehicle navigation pipeline*, which 1) captures an image from Gazebo in the current vehicle state and environment, 2) passes the image through the neural network to get the approximate perceived state, 3) calculates a steering angle based on the *perceived state*, and 4) calculates the position of the vehicle after one time step using the *actual state* and steering angle. At each time step, we calculate the fraction of vehicles remaining within the safe region.

Unfortunately, MCS requires a large amount of time. The major contributor to runtime is image generation using Gazebo and processing using the neural network. Furthermore, if we increase the number of samples for more confidence, or increase the number of time steps, the simulation time increases proportionally.

2.1 GAS: Using Generalized Polynomial Chaos

To reduce analysis time, we use GPC to construct a polynomial model as a replacement for the original navigation model. Constructing the GPC model requires evaluating the navigation model a small number of times (< 1000), independent of the number of distribution estimation samples or time steps. Unfortunately, small changes in the input image to the neural network can greatly affect its output, which affects the final state of the vehicle – this is something that a GPC polynomial model cannot accurately replicate.

Perception Model. We present GAS, a novel approach for constructing polynomial models of navigation systems and using them for state distribution estimation. First, GAS creates an abstract navigation model by replacing Gazebo image generation and neural network processing with a *perception model*. To train the perception model, we choose 121 ground truth states in a 11 by 11 grid in the safe region. At each ground truth state, we gather 350 images with randomly sampled environmental conditions, pass them through the neural network, and store the outputs. GAS assumes that, for any given heading h and distance d , the output of the neural network is drawn from a 2D normal distribution with mean vector $\mu(h, d)$ and the covariance matrix $\sigma^2(h, d)$. GAS uses the 350 outputs for each ground truth state to calculate μ and σ^2 for that state, and trains a degree 4 polynomial regression model to predict μ and σ^2 for any state

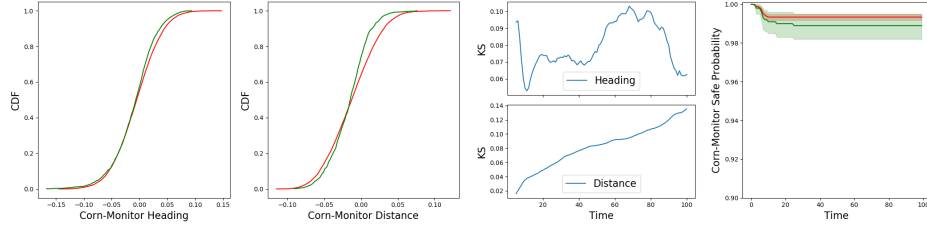


Fig. 5: Distributions at final time step

Fig. 6: Distribution similarity over time

Fig. 7: Safe probabilities over time

in the safe region. Instead of returning the state perceived by the neural network, this perception model returns the *distribution* of possible perceived states. GAS samples this perceived state distribution when constructing the GPC model of the entire navigation system.

GPC Model Construction. Next, GAS next creates an abstract navigation model which accepts a sample from a standard normal distribution instead of an environment (bottom half of Figure 4). The abstracted navigation model first calculates the neural network output distribution parameters using the perception model, then transforms the raw input sample into a sample from this output distribution. The navigation model uses this sample for the rest of the pipeline.

To construct the GPC model, GAS 1) creates a joint distribution, consisting of a distribution over all safe vehicle states and the standard normal distribution used by the abstracted vehicle model, 2) chooses a set of polynomials which are orthogonal w.r.t. the joint distribution, 3) picks specific samples from the joint distribution that are necessary for *Gaussian quadrature*, a fast and accurate numerical integration method, 4) evaluates these samples with the abstracted navigation model, and finally 5) uses the input samples and the corresponding outputs to create the polynomial model of the end to end vehicle navigation system. The GAS model is a 4th degree polynomial over 4 state variables with 70 terms, including 53 interaction terms. GAS substitutes this model in place of the original navigation model in the MCS procedure described above to estimate the state distribution of the vehicle over time. Since the GAS model is faster than the original model, GAS increases the number of simulations to 10000 for higher fidelity distribution estimation.

2.2 Results

Accuracy. Figure 5 shows a comparison of the heading and distance distributions after 100 time steps. The X Axis shows the variable value and the Y Axis shows the cumulative probability. The green and red plots show the distributions estimated using MCS and GAS, respectively. We compare the GAS and MCS distributions using the Kolmogorov-Smirnov (KS) statistic, which is a conservative measure of distribution similarity, and the Wasserstein metric. Figure 6

shows how the KS statistic evolves over time. The X Axis shows time steps and the Y Axis shows the KS statistic. The low KS statistic value indicates good correlation between the two distributions at all times. The Wasserstein metric also remains below 0.02. Figure 7 shows the probability of remaining in a safe state over time. The X Axis shows time steps and the Y Axis shows the probability of remaining safe. The shaded region around each plot shows the 95% bootstrap confidence interval. We use the t-test to check if the safe state probabilities are similar. The t-test passes for 99 of 100 time steps, indicating high similarity.

Time. GAS is 2.3x faster than MCS. MCS required 19.5 hours on our hardware. Gathering the training data for the perception model required 8.5 hours on our hardware. The time required for training the perception model, constructing the polynomial approximation with GPC, and using the GPC approximation was negligible in comparison (< 1 minute). Increasing the number of samples or the number of time steps would further increase the gap between the two methods.

Conclusion. These results jointly indicate that GAS gives us a faster, accurate replacement for MCS of this autonomous corn row navigation model.

3 Background

We present key GPC definitions. Dedicated books, e.g., [31], give more details.

Lagrange Basis Polynomials. Given points

$$(x_i, y_i), 1 \leq i \leq N, \text{ where all } x_i \text{ are distinct, } L_i(x) = \prod_{\substack{1 \leq j \leq N \\ j \neq i}} \frac{x - x_j}{x_i - x_j} \quad (1)$$

Equation 1 gives the *Lagrange basis polynomials* L_i for this set of points.

Orthogonal Polynomials. Assume X is a continuous variable with support S_X and p.d.f. $p_X : S_X \rightarrow \mathbb{R}$. Let $\Psi = \{\Psi_n | n \in \mathbb{N}_0\}$ be a set of polynomials, where Ψ_n is an n^{th} degree polynomial. Then Ψ is a set of orthogonal polynomials with respect to X if $n \neq m \Rightarrow \int_{S_X} \Psi_n(x) \Psi_m(x) p_X(x) dx = 0$. The orthogonal polynomial Ψ_n has n distinct roots in S_X .

Orthogonal Polynomial Projection (GPC). Let $f : S_X \rightarrow \mathbb{R}$. Then the N^{th} order orthogonal polynomial projection of f , written as f_N , with respect to a set of orthogonal polynomials Ψ , is:

$$f_N = \sum_{i=0}^N c_i \Psi_i \quad \text{where} \quad c_i = \frac{\int_{S_X} f(x) \Psi_i(x) p_X(x) dx}{\int_{S_X} \Psi_i^2(x) p_X(x) dx}, \quad (2)$$

If f is a N^{th} degree polynomial, then $f_N = f$. Otherwise, f_N is the *optimal* N^{th} degree polynomial approximation of f w.r.t. X , in the sense that it minimizes ℓ_2 error, calculated as $\int_{S_X} (f(x) - f_N(x))^2 p_X(x) dx$. The ℓ_2 error is lower for functions that are close in behavior to an N^{th} degree polynomial. As N approaches ∞ , the ℓ_2 error approaches 0, meaning that we can construct arbitrarily good approximations of f . f_N is called the N^{th} -order generalized polynomial chaos

(GPC) approximation. GPC can be easily extended for functions of multiple *independent* variables. We provide details in Appendix A.

Gaussian Quadrature. To use Equation 2, we must perform multiple integrations to calculate the coefficients c_i ($i \in \{0 \dots N\}$). For any non-trivial function g , we must use numerical integration by approximating the integral with a sum:

$$\int_{S_X} g(x)p_X(x)dx \approx \sum_{i=1}^N w_i g(x_i) \quad \text{where} \quad w_i = \int_{S_X} L_i(x)p_X(x)dx \quad (3)$$

We choose w_i and x_i so as to minimize integration error. In *Gaussian quadrature*, we choose x_i to be the N roots of Ψ_N , the N^{th} order orthogonal polynomial w.r.t. X . We calculate the corresponding weights using the Lagrange basis polynomials L_i (Equation 1) passing through $x_j \forall j \neq i$.

Global Sensitivity (Sobol) Indices. Sobol Indices [29] decompose the variance of the model output over the entire input distribution into portions that depend on subsets of the input variables. Particularly, the *first order* sensitivity indices show the contribution of a single input variable to the output variance. For an input variable X_i , the sensitivity index $S_i = V_i/V$, where $V = \text{Var}_{\mathbf{X}}(f(\mathbf{x}))$ is the total variance and $V_i = \text{Var}_{X_i}(E_{\mathbf{X}_{\sim i}}(f(\mathbf{x})|x_i))$. Here $\mathbf{X}_{\sim i}$ is the set of all input variables except X_i .

4 GAS Approach

We present our approach for estimating the state distribution over time for a vehicle navigation system containing an image processing neural network. GAS consists of four high level steps:

1. Create a deterministic end-to-end vehicle navigation model.
2. Train a perception model (Algorithm 1) and use it to replace the neural network in the vehicle model (Algorithm 2).
3. Construct a GPC polynomial model from the vehicle model (Algorithm 3).
4. Use the GPC polynomial model for estimating the state distribution and safe state probability over time (Algorithm 4).

GAS automates almost the entire process of constructing and using the GPC model. The user provides the perception model training data, the distributions of state and random variables, GPC order, and simulation parameters. GAS infers the optimal degree of polynomial regression for the perception model using cross-validation to maximize accuracy while preventing overfitting.

4.1 Creating a Deterministic Vehicle Model

First, we represent the end-to-end vehicle model as a function of independent random variables, $M_V : \mathbb{D}_S \times \mathbb{D}_E \times \mathbb{D}_R \rightarrow \mathbb{D}_S$. $S \in \mathbb{D}_S$ is a vector of state variables, $E \in \mathbb{D}_E$ is a vector of environment-related random variables that affect

the neural network, and $R \in \mathbb{D}_R$ is a vector of random variables that do not affect the neural network, but affect other parts of M_V . Making M_V deterministic is necessary as GPC produces a deterministic polynomial model over independent random variables. Because multivariate GPC requires the input variables to be independent, we remove any input variable dependencies by isolating their independent components and using those as the input variables instead.

4.2 Replacing Image Processing Components

Polynomials over reals are continuous and have a limited number of inflection points. Consequently, polynomials make poor replacements for models that are discontinuous or whose output changes rapidly with small changes in input. Image processing neural networks are particularly susceptible to perturbations – even tiny changes in the input image can lead to significant output changes [24].

This is why GAS replaces the neural network with a perception model prior to constructing the GPC polynomial model. Algorithm 1 shows how GAS creates the perception model. The steps are as follows:

1. Suppose \mathbb{D}_S^S is the safe set of states. We pick a set of ground truth states $G \subset \mathbb{D}_S^S$, such that G is an evenly spaced tensor grid that includes the extreme states within \mathbb{D}_S^S .
2. For each $g \in G$, GAS captures a list of images I_g using a photorealistic simulator such as Gazebo and AirSim. For each image, GAS randomly samples E from the environment distribution \mathcal{D}_E ($E \sim \mathcal{D}_E$). GAS obtains a large number of images per state ($N_i \geq 350$) to get a high confidence estimate of the output distributions in the next step.
3. For each $g \in G$, GAS passes I_g through the neural network to obtain a list of network outputs O_g . GAS calculates the mean μ_g and covariance σ_g^2 of O_g .
4. GAS trains a polynomial regression model M_{per} to predict μ_S and σ_S^2 for any $S \in \mathbb{D}_S^S$.

The perception model M_{per} returns a *distribution* of possible outputs. We create an *abstracted* vehicle model $M'_V : \mathbb{D}_S \times \mathbb{R}^n \times \mathbb{D}_R \rightarrow \mathbb{D}_S$ (Algorithm 2) to use M_{per} instead of the neural network. Instead of a sample from \mathcal{D}_E , M'_V accepts a sample N from a multivariate standard normal distribution $\mathcal{N}(0, 1)$. It calculates μ_S and σ_S^2 using M_{per} , and transforms N to a sample from $\mathcal{N}(\mu_S, \sigma_S)$. M'_V uses this sample as the neural network output for the rest of the model.

We assume the output is distributed according to $\mathcal{N}(\mu_S, \sigma_S)$ as we can easily define the distribution in terms of μ_S, σ_S^2 . However, we can use any distribution whose parameters we can predict through polynomial regression. Likewise, instead of choosing raw samples from $\mathcal{N}(0, 1)$, we can sample any distribution that has orthogonal polynomials for use with GPC (e.g., Uniform, Beta, or more complicated distributions as polynomials of such random variables).

4.3 GPC for the End to End Vehicle System

Algorithm 3 shows how GAS constructs the GPC approximation of the abstracted vehicle model:

Algorithm 1 Training the perception model

Input G : even, extensive tensor grid in safe state space; \mathcal{D}_E : distribution of environment variables; N_i : number of images to capture for each $g \in G$
Returns M_{per} : trained perception model

```

1: function TRAINPERCEPTIONMODEL( $G, \mathcal{D}_E, N_i$ )
2:    $TrainTestData \leftarrow \{ \}$ 
3:   for  $g \in G$  do
4:      $I_g \leftarrow []$ 
5:     for  $i$  from 1 to  $N_i$  do
6:        $E \sim \mathcal{D}_E$ 
7:        $Img \leftarrow \text{CAPTUREIMAGE}(g, E)$ 
8:        $I_g \leftarrow I_g :: Img$ 
9:      $O_g \leftarrow \text{NEURALNETWORK}(I_g)$ 
10:     $\mu_g \leftarrow \text{MEAN}(O_g)$ 
11:     $\sigma_g^2 \leftarrow \text{COVARIANCE}(O_g)$ 
12:     $TrainTestData \leftarrow TrainTestData[g \mapsto (\mu_g, \sigma_g^2)]$ 
13:   $M_{per} \leftarrow \text{POLYNOMIALREGRESSIONMODEL}(TrainTestData)$ 

```

Algorithm 2 Abstracted vehicle model

Input S : initial state of vehicle; N : raw sample to be transformed into neural network output sample; R : other random variables; M_{per} : trained perception model
Returns S' : state of vehicle after one time step

```

1: function  $M'_V(S, N, R, M_{per})$ 
2:    $\mu_S, \sigma_S^2 \leftarrow M_{per}(S)$ 
3:    $O_S \leftarrow \text{TRANSFORM}(N, \mu_S, \sigma_S^2)$ 
4:    $S' \leftarrow \text{VEHICLECONTROLANDDYNAMICS}(S, O_S, R)$ 

```

1. GAS constructs a joint distribution J over $\mathbb{D}_S \times \mathbb{R}^n \times \mathbb{D}_R$. For the state variables, GAS chooses a normal or truncated normal distribution \mathcal{D}_S^S over the safe state space \mathbb{D}_S^S . GAS uses $\mathcal{N}(0, 1)$ for the perception model raw sample. For the other random variables, GAS uses their actual distribution \mathcal{D}_R .
2. GAS constructs the basis polynomials which are orthogonal w.r.t. J . Increasing the order o_{gpc} increases accuracy, but also runtime.
3. GAS chooses samples from J and calculates the corresponding weights for using Gaussian quadrature using Equation 3.
4. GAS evaluates the abstracted vehicle model M'_V at the chosen samples.
5. GAS calculates the GPC polynomial model as the weighted sum of the orthogonal polynomials using Equation 2.

Algorithm 4 shows how GAS uses the GPC model to estimate the probability that the vehicle will remain in a safe state over time. GAS creates initial joint samples using the initial state distribution \mathcal{D}_S^0 , the raw sample distribution, and the distribution of other random variables (Line 4). At each time step, GAS evaluates the GPC model on each joint sample to get the next state. If the next state is safe, GAS chooses new random values to prepare the joint sample for the next time step. Finally, GAS calculates and stores the fraction of samples that are still in the safe region.

Algorithm 3 GPC approximation construction

Input \mathcal{D}_S^S : distribution over \mathbb{D}_S^S ; \mathcal{D}_R : distribution of other random variables; o_{gpc} : order of GPC model; M'_V : abstracted vehicle model
Returns M_{GPC} : GPC polynomial model

- 1: **function** CREATEGPCMODEL($\mathcal{D}_S^S, \mathcal{D}_R, o_{gpc}, M'_V$)
- 2: $J \leftarrow \text{JOIN}(\mathcal{D}_S^S, \mathcal{N}(0, 1), \mathcal{D}_R)$
- 3: $\Psi \leftarrow \text{GENERATEORTHOGONALPOLYNOMIALS}(order = o_{gpc}, J)$
- 4: $X, W \leftarrow \text{GENERATEQUADRATURENODESANDWEIGHTS}(order = o_{gpc}, J)$
- 5: $Y \leftarrow [M'_V(x) \text{ for } x \in X]$
- 6: $M_{GPC} \leftarrow \text{QUADRATUREANDGPC}(\Psi, X, W, Y)$

Computing Sobol Indices. Because variable marginalization and analytical integration is simple for polynomials, GAS can analytically calculate the Sobol indices for M_{GPC} over the joint distribution J . To calculate Sobol indices using MCS, we have to use estimators that increase in accuracy as the number of samples increases.

Algorithm 4 Using the GPC approximation to estimate safe probability

Input N_s : number of samples to use for distribution estimation; T : number of time steps; \mathcal{D}_S^0 : initial state distribution; \mathcal{D}_R : distribution of other random variables; $Pred$: safety predicate; M_{GPC} : constructed GPC approximation
Returns P_{safe} : probability that the vehicle is safe until each time step

- 1: **function** ESTIMATESAFEPROBABILITY($N_s, T, \mathcal{D}_S^0, \mathcal{D}_R, Pred, M_{GPC}$)
- 2: $X \leftarrow []$; $P_{safe} \leftarrow \{ \}$
- 3: **for** i from 1 to N_s **do**
- 4: $x \sim \text{JOIN}(\mathcal{D}_S^0, \mathcal{N}(0, 1), \mathcal{D}_R)$
- 5: $X \leftarrow X :: x$
- 6: **for** t from 1 to T **do**
- 7: $X' \leftarrow []$
- 8: **for** $x \in X$ **do**
- 9: $S' \leftarrow M_{GPC}(x)$
- 10: **if** $\text{SAFE}(S', Pred)$ **then**
- 11: $N' \sim \mathcal{N}(0, 1)$
- 12: $R' \sim \mathcal{D}_R$
- 13: $X' \leftarrow X' :: (S', N', R')$
- 14: $X \leftarrow X'$
- 15: $P_{safe} \leftarrow P_{safe}[t \mapsto |X|/N_s]$

Accuracy. Multiple GAS parameters affect the accuracy of the GPC model: the tensor grid size $|G|$, the number of images for each grid point N_i , the degree of polynomial regression used for the perception model, and the GPC order o_{gpc} . Under certain conditions, GAS converges in distribution to the exact solutions.

Theorem 1 (GAS Convergence). *Assume that for a particular environment distribution \mathcal{D}_E , the distribution of neural network outputs in any state is Gaussian. Then, the GAS model M_{GPC} converges in output distribution to the original vehicle model M_V .*

We provide a proof sketch for Theorem 1 in Appendix B.

Runtime. The most time consuming components of the vehicle model are photorealistic image capture and subsequent neural network image processing. MCS requires $\Theta(N_s T)$ evaluations of these components, while GAS requires $\Theta(|G| N_i)$ evaluations. GAS also requires additional time for training M_{per} , constructing M_{GPC} , and $\Theta(N_s T)$ evaluations of M_{GPC} . As a result, the speedup offered by GAS – after amortizing the GPC creation time – depends strongly on the speedup of M_{GPC} over the original vehicle model M_V used for MCS.

Scalability. The GPC polynomial model must consider all possible interactions between state variables, and can suffer from the “curse of dimensionality” (combinatorial explosion of the number of polynomial terms). This is a general GPC limitation, for which researchers in engineering applications have proposed, e.g., low-rank approximation [18], or a combination of GPC and MCS [25]. The authors of the former approach successfully apply it to a scenario with over 50 input random variables (parameters). These are interesting directions for future research, but are beyond the scope of GAS.

Vehicle models with categorical state variables. GAS uses Multi-Element GPC (MEGPC) for vehicle models that have categorical state variables, in conjunction with an *ancillary model* for predicting the final values of the categorical state variables. Details of this approach are provided in Appendix C.

5 Methodology

Benchmarks. We chose five benchmarks that include autonomous vehicle systems such as self driving cars, aerial drones, and crop monitoring vehicles. Table 1 shows details of the benchmarks. Columns 2 and 3 state the vehicle’s perception and control system, respectively. Columns 4 and 5 state the number of state dimensions and random variable dimensions, respectively. Column 6 indicates if GAS made a replacement in the perception (Perc) or control (Ctrl) system, and the nature of the replacement (Poly Reg: polynomial regression, Dec Tree: decision tree). The benchmarks are:

- **Corn Monitoring Vehicle.** A vehicle that travels between two rows of corn and must avoid hitting them. This is our main example (Section 2).
- **Self-Driving Car on a Straight Road.** A vehicle that must drive within a road lane ($\mathbb{D}_S^S \equiv |\text{heading}| \leq \pi/12 \wedge |\text{distance}| \leq 1.2m$). It uses LaneNet to

Table 1: GAS benchmarks

Benchmark	Perception	Control	dim _s	dim _r	Replacement
Corn-Monitor	Resnet-18	Skid-Steer	2	2	Perc \rightarrow Poly Reg
Car-Straight	LaneNet	Pure Pursuit	2	2	Perc \rightarrow Poly Reg
Car-Curved	LaneNet	Pure Pursuit	2	2	Perc \rightarrow Poly Reg
ACAS-Table	Ground Truth	ACAS-Xu Table	4	0	Ctrl \rightarrow Dec Tree
ACAS-NN	Ground Truth	ACAS-Xu NN	4	0	Ctrl \rightarrow Dec Tree

perceive the location of the lane edges and uses the pure pursuit controller. We derive this benchmark from [7].

- **Self-Driving Car on a Curved Road.** Similar to the previous benchmark, but on a circular road of 100m radius.
- **Aerial Drone Collision Avoidance (Lookup Table).** An aerial drone that must avoid a near miss with an intruder ($\mathbb{D}_S^S \equiv |\text{separation}| \geq 500\text{ft}$). The drone uses ACAS-Xu lookup tables from [15]. As this model’s state includes a categorical variable (the previous ACAS advisory), we use MEGPC and predict the next advisory using a decision tree.
- **Aerial Drone Collision Avoidance (Neural Network).** Similar to the previous benchmark, but uses a neural network from [15] trained to replace the lookup table. We use decision tree for predicting the next advisory.

Implementation and Experimental Setup. We performed our experiments on machines with an Intel Xeon CPU, NVIDIA Quadro P5000 GPU, 32 GB RAM, and Ubuntu 20.04. We implement GAS in Python, using the chaospy library [10]. We use Gazebo 11 [17] to capture images for Corn-Monitor, Car-Straight, and Car-Curved benchmarks. We run all image processing neural networks on the GPU. We run ACAS-NN entirely on CPU as its network is small.

Since there are no closed form solutions for calculating the state distribution over time for non-trivial systems, we compare GAS to a MCS baseline. We set GAS parameters as follows: G is a 11x11 grid in the safe state space, $N_i = 350$, and $o_{gpc} = 4$. We set the number of time steps $T = 100$. For MCS, we set $N_s = 1000$ to limit runtime to ≤ 24 hours. For GAS, we set $N_s = 10000$ for better distribution fidelity and confidence bounds.

Distribution Similarity Metrics. We use two complementary similarity metrics to compare MCS and GAS state distributions at each time step. The KS statistic quantifies the maximum distance between two cumulative distribution functions, while the Wasserstein metric can be interpreted as the energy needed to transform one distribution into another. The smaller the metrics are, the more closely the two distributions resemble each other. We also compare the fraction of simulated vehicles remaining in the safe region till each time step.

6 Evaluation

6.1 Does GAS provide an *accurate* replacement for Monte Carlo Simulation of end to end vehicle systems?

Table 2 presents the values of the distribution similarity metrics. For each benchmark state variable, Columns 3-4 show the maximum values of the KS statistic and Wasserstein metric over all time steps. The Wasserstein metric is high for the distance variables of the ACAS benchmarks due to their large range. However, the metric is still low compared to the variance of these variables. Columns 5-6 compare the mean and standard deviation of the distributions at the final time step, showing that they are close. We also visualize the distributions in the final time step in Appendix D.

Table 2: State variable distribution comparison

Benchmark	Variable	KS_{\max}	$Wass_{\max}$	$\mu_{\text{GAS}}/\mu_{\text{MCS}}$	$\sigma_{\text{GAS}}/\sigma_{\text{MCS}}$
Corn-Monitor	Heading (rad)	0.11	0.02	0.00/-0.01	0.04/0.04
	Distance (m)	0.14	0.01	-0.01/-0.02	0.03/0.03
Car-Straight	Heading (rad)	0.09	0.00	0.00/0.00	0.01/0.01
	Distance (m)	0.12	0.02	0.09/0.10	0.05/0.06
Car-Curved	Heading (rad)	0.17	0.00	0.00/0.00	0.01/0.01
	Distance (m)	0.12	0.01	0.05/0.06	0.04/0.05
ACAS-Table	Crossrange (ft)	0.06	155	-845/-985	1424/1458
	Downrange (ft)	0.04	116	2224/2113	1751/1702
	Heading (rad)	0.02	0.05	0.15/0.17	1.71/1.69
ACAS-NN	Crossrange (ft)	0.09	382	869/489	1753/1943
	Downrange (ft)	0.05	138	2154/2019	1658/1646
	Heading (rad)	0.02	0.05	-0.07/-0.04	1.73/1.76

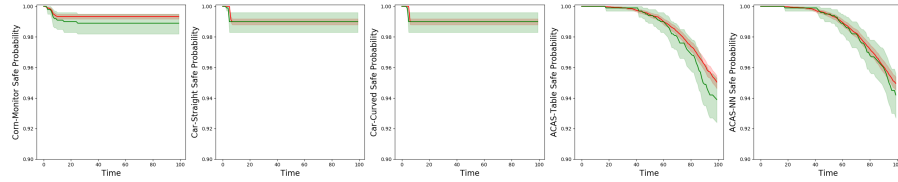


Fig. 8: Evolution of safe state probability over time. Red: GAS, Green:MCS.

Figure 8 shows the time evolution of the probability that the vehicle remains in a safe state. The red plots show the probability estimate obtained using GAS, while the green plots show the probability estimate obtained using MCS. The shaded region around each plot shows the 95% bootstrap confidence interval. Since GAS approximates the behavior of the vehicle model, as opposed to under/over approximation of reachable states, GAS’s safe state probability estimate can be on either side of the MCS estimate.

Table 3: Safe state probability comparison

Benchmark	t-test pass	ℓ_2 error	X-Cor
Corn-Monitor	99/100	0.004	0.974
Car-Straight	99/100	0.001	0.905
Car-Curved	99/100	0.001	0.907
ACAS-Table	100/100	0.051	0.998
ACAS-NN	100/100	0.021	0.998

Table 3 shows the metrics we use to rigorously measure the similarity of the safe state probabilities from Figure 8. We used the standard t-test to analyze the similarity of the safe state probabilities computed by GAS and MCS in each time step. Column 2 shows the number of time steps for which the t-test “passed”, meaning that we could not reject the null hypothesis that the probabilities are equal. Column 3 shows the ℓ_2 error – RMS of the differences in

Table 4: Time usage comparison for GAS and MCS (*use same ancillary model).

Benchmark	t_{MCS}	t_{model}	t_{GPC}	Speedup	$t_{sens}^{MCS}/N_s^{sens}$	t_{sens}^{GPC}	Speedup
Corn-Monitor	19.5h	8.5h	3.4s	2.3×	99.9s/10 ⁷	12.3s	8.1×
Car-Straight	4.9h	1.9h	3.1s	2.6×	102s/10 ⁷	12.5s	8.2×
Car-Curved	4.9h	1.9h	3.2s	2.6×	99.6s/10 ⁷	11.7s	8.5×
ACAS-Table	7.7s	0.29s*	3.1s	2.3×	394s/10 ⁶	3.3s	119.4×
ACAS-NN	10.3s	0.29s*	3.2s	3.0×	516s/10 ⁶	3.4s	151.8×

safe state probability at each time step, and Column 4 shows the cross-correlation – the Pearson correlation coefficient between the two series of probabilities. The similarity of the safe state probability is directly the result of the similarity of the state distributions.

In conclusion, the vehicle state variable distributions that we estimate using GAS closely resemble those that we estimate using MCS, even after 100 time steps. Consequently, the vehicle safe state probability estimate is also similar between the two approaches.

6.2 Is GAS faster compared to Monte Carlo Simulation?

Table 4 compares the time required for distribution estimation using MCS (Column 2) and GAS (Columns 3-4). Column 3 gives the time required to gather data for and train the perception model and/or the ancillary model. Column 4 gives the time required for constructing and using the GPC model. Finally, Column 5 gives the relative speedup of GAS over MCS.

The time consuming process of gathering images using Gazebo and processing them with the neural network leads to the high time requirement for the Corn-Monitor, Car-Straight, and Car-Curved benchmarks, both for MCS and for gathering the training data for the perception model. Increasing N_s or T increases t_{MCS} , but not t_{model} . Consequently, the speedup of GAS increases for longer experiments or higher number of samples. Constructing and using the GPC approximation takes a comparatively negligible amount of time. The ACAS-Table and ACAS-NN benchmarks require less time as their models are much simpler. Even then, GAS provides a speedup over the MCS approach, while having 10× the samples.

Reducing perception model parameters such as N_i and the size of G leads to further speedups. However, we observed that such changes caused significant reduction in accuracy. We describe these observations in detail in Appendix E.

In conclusion, GAS provides 2.3× to 3.0× speedups over MCS, despite the additional time required to construct the perception and/or ancillary model and using ten times more samples than MCS for distribution estimation.

6.3 Can the GAS model be used for fast global sensitivity analysis?

Using the GAS polynomial model, we analytically calculate the first order Sobol sensitivity indices for the model, as opposed to calculating them using MCS.

Figure 9 shows how one of the first order sensitivity indices for Corn-Monitor calculated using MCS approaches the value calculated analytically using the GAS model. The X-Axis shows the number of simulations, while the Y-Axis shows the index value. Figure 9 shows that 10^6 - 10^7 runs are required to accurately calculate sensitivity indices with MCS. Given the cost of running the original vehicle model M_V , for sensitivity analysis with MCS, we use the abstracted vehicle model M'_V . We present the rest of the sensitivity index plots like Figure 9 in Appendix F.

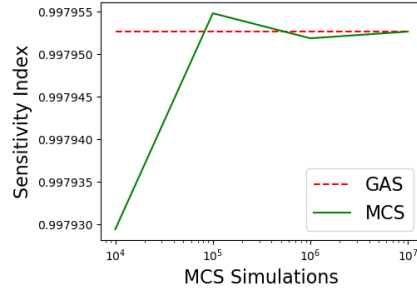


Fig. 9: Sensitivity Index Comparison

Table 4 Column 6 shows the time taken to calculate all first order sensitivity indices using MCS and the number of samples used. Column 7 shows the corresponding times for GAS and Column 8 shows the speedup from 8x-150x.

In conclusion, the GAS model is also a superior alternative to MCS for calculating the sensitivity indices of the vehicle model.

7 Related Work

Simulation and modeling of systems. Althoff et al. [2] model multi-vehicle scenarios using MCS and Markov Chain models. The Markov Chain approach suffers from discretization error, while MCS requires many samples. GAS does not suffer from either of these problems. Kewlani et al. [16] use GPC for analyzing the effects of vehicle *dynamics* components on the vehicle state. GAS extends the applicability of GPC to end-to-end vehicle systems with complex components.

Most classical system identification techniques handle only linear systems. Recently, ARIsTEO [21] used system identification to reduce the cost of testing cyber-physical systems. Recent techniques that use ML to address nonlinearity are typically unsuitable for characterizing model uncertainty. In contrast, GPC both captures model non-linearity and efficiently propagates uncertainty.

Simplification of complex perception and control systems. Cheng et al. [4] explore the correspondence between a neural network and polynomial regressions. Unlike their approach, our perception model only needs to predict

the *distribution* of neural network outputs, instead of individual input-output relationships. Multiple works construct and verify neural network alternatives to the ACAS-Xu lookup tables [15,30]. Our benchmarks use both the lookup table and neural network. Compared to verification, estimating the distribution of states using GPC takes only a few seconds. Hsieh et al. [13] create a perception model using piecewise linear regression, and verify the perception model composed with downstream components using model checking tools such as CBMC. In contrast, our perception model uses polynomial regression, and estimates safe state probabilities using GPC.

Formal verification of vehicle systems. DryVR [9] verifies the safety of vehicle models that have a whitebox mode-switching control system with a blackbox dynamics system. GAS supports models with perception neural networks, which act like blackbox control systems due to their uninterpretability. Researchers have extensively explored the problem of formal verification of vehicle related systems [3,5,12,14,19,23,26]. Many of these techniques suffer from either a lack of flexibility or scalability (e.g., can be applied only at a component-level). Recently, probabilistic analysis techniques started to address these concerns for entire systems and/or individual components [1,6,11,20]. GAS can provide accurate reliability estimates for a wide variety of complex vehicle systems whose simulations and analyses are time-consuming.

8 Conclusion

We present GAS, the first methodology for using Generalized Polynomial Chaos (GPC) to analyze a complete autonomous vehicle navigation system. GAS 1) creates an analyzable model of the perception subsystem and 2) uses it to generate a GPC model of the entire system pipeline. GAS accurately models the system while being 2.3x-3.0x faster than Monte Carlo Simulation on five scenarios used in agricultural vehicles, self driving cars, and aerial drones. These results indicate an exciting unexplored potential for GPC and similar techniques in analysis of autonomous systems. We anticipate future intersection with symbolic formal methods to jointly improve system reliability.

References

1. Abbas, H., Fainekos, G., Sankaranarayanan, S., Ivancic, F., Gupta, A.: Probabilistic temporal logic falsification of cyber-physical systems. *TECS* **12** (2013)
2. Althoff, M., Mergel, A.: Comparison of markov chain abstraction and monte carlo simulation for the safety assessment of autonomous cars. *T-ITS* **12** (2011)
3. Aniculaesei, A., Arnsberger, D., Howar, F., Rausch, A.: Towards the verification of safety-critical autonomous systems in dynamic environments. *EPTCS* **232** (2016)
4. Cheng, X., Khomtchouk, B., Matloff, N., Mohanty, P.: Polynomial regression as an alternative to neural nets (2019)
5. Clarke, E., Fehnker, A., Han, Z., Krogh, B., Stursberg, O., Theobald, M.: Verification of hybrid systems based on cegar. In: *TACAS* (2003)

6. Converse, H., Filieri, A., Gopinath, D., Pasareanu, C.S.: Probabilistic symbolic analysis of neural networks. In: ISSRE (2020)
7. Du, P., Huang, Z., Liu, T., Ji, T., Xu, K., Gao, Q., Sibai, H., Driggs-Campbell, K., Mitra, S.: Online monitoring for safe pedestrian-vehicle interactions. In: ITSC (2020)
8. Ernst, O., Mugler, A., Starkloff, H.J., Ullmann, E.: On the convergence of generalized polynomial chaos expansions. *ESAIM: Mathematical Modelling and Numerical Analysis* **46** (2012)
9. Fan, C., Qi, B., Mitra, S., Viswanathan, M.: Dryvr: Data-driven verification and compositional reasoning for automotive systems. In: CAV (2017)
10. Feinberg, J., Langtangen, H.P.: Chaospy: An open source tool for designing methods of uncertainty quantification. *Journal of Com. Sci.* **11** (2015)
11. Filieri, A., Pasareanu, C.S., Visser, W., Geldenhuys, J.: Statistical symbolic execution with informed sampling. In: FSE (2014)
12. Gros, T.P., Hermanns, H., Hoffmann, J., Klauck, M., Steinmetz, M.: Deep statistical model checking. In: FORTE (2020)
13. Hsieh, C., Li, Y., Sun, D., Joshi, K., Misailovic, S., Mitra, S.: Verifying controllers with vision-based perception using safe approximate abstractions. In: EMSOFT (2022)
14. Jha, S.K., Krogh, B.H., Weimer, J.E., Clarke, E.M.: Reachability for linear hybrid automata using iterative relaxation abstraction. In: HSCC (2007)
15. Julian, K.D., Kochenderfer, M.J.: Guaranteeing safety for neural network-based aircraft collision avoidance systems. In: DASC (2019)
16. Kewlani, G., Crawford, J., Iagnemma, K.: A polynomial chaos approach to the analysis of vehicle dynamics under uncertainty. *Veh. Sys. Dyn.* **50** (2012)
17. Koenig, N., Howard, A.: Design and use paradigms for gazebo, an open-source multi-robot simulator. In: IROS (2004)
18. Konakli, K., Sudret, B.: Uncertainty quantification in high-dimensional spaces with low-rank tensor approximations. In: UNCECOMP (2015)
19. Larsen, K.G., Mikučionis, M., Taankvist, J.H.: Safe and Optimal Adaptive Cruise Control, pp. 260–277. Springer (2015)
20. Mangal, R., Nori, A.V., Orso, A.: Robustness of neural networks: A probabilistic and practical approach. In: ICSE-NIER (2019)
21. Menghi, C., Nejati, S., Briand, L., Parache, Y.I.: Approximation-refinement testing of compute-intensive cyber-physical models: An approach based on system identification. In: ICSE (2020)
22. Pan, R., Rajan, H.: On decomposing a deep neural network into modules. In: Proceedings of the 28th ACM Joint Meeting on European Software Engineering Conference and Symposium on the Foundations of Software Engineering (2020)
23. Păsăreanu, C.S., Gopinath, D., Yu, H.: Compositional Verification for Autonomous Systems with Deep Learning Components, pp. 187–197. Springer (2019)
24. Pei, K., Cao, Y., Yang, J., Jana, S.: Deepxplore: Automated whitebox testing of deep learning systems. *Commun. ACM* **62** (2019)
25. Poëtte, G.: A gpc-intrusive monte-carlo scheme for the resolution of the uncertain linear boltzmann equation. *Journal of Computational Physics* **385** (2018)
26. Prabhakar, P., Duggirala, P.S., Mitra, S., Viswanathan, M.: Hybrid automata-based cegar for rectangular hybrid systems. In: VMCAI (2013)
27. Robert, C.P., Casella, G.: Monte Carlo statistical methods, vol. 2. Springer (2004)
28. Sivakumar, A.N., Modi, S., Gasparino, M.V., Ellis, C., Velasquez, A.E.B., Chowdhary, G., Gupta, S.: Learned visual navigation for under-canopy ag robots (2021)

29. Sobol, I.: Global sensitivity indices for nonlinear mathematical models and their monte carlo estimates. *Mathematics and Computers in Simulation* **55** (2001)
30. Tran, H.D., Yang, X., Manzanas Lopez, D., Musau, P., Nguyen, L.V., Xiang, W., Bak, S., Johnson, T.T.: Nnv: The neural network verification tool for deep neural networks and learning-enabled cyber-physical systems. In: *CAV* (2020)
31. Xiu, D.: *Numerical Methods for Stochastic Computations: A Spectral Method Approach*. Princeton University Press (2010)

A Multivariate GPC

Multivariate GPC. GPC can be easily extended to the multivariate case, as long as all *all random variables are independent*. Let $\mathbf{X} = X_1, \dots, X_d$ be the d independent random variables and let f be a function over \mathbf{X} . The orthogonal polynomials Ψ_i for \mathbf{X} are simply the products of the orthogonal polynomials $\Psi_{i_1}, \dots, \Psi_{i_d}$ for X_1, \dots, X_d respectively. The GPC approximation closely resembles the one for the univariate case:

$$f_N = \sum_i c_i \Psi_i \quad \text{where} \quad c_i = \frac{\int f(\mathbf{x}) \Psi_i(\mathbf{x}) p_{\mathbf{X}}(\mathbf{x}) d\mathbf{x}}{\int \Psi_i^2(\mathbf{x}) p_{\mathbf{X}}(\mathbf{x}) d\mathbf{x}} \quad (4)$$

We calculate c_i , using Gaussian quadrature, in a manner analogous to the univariate case, but summing over all dimensions of \mathbf{i} .

B Proof Sketch: GAS Convergence

Lemma 1 (GPC Error Bound). *The root mean square (RMS) error of the outputs of the GAS model M_{GPC} with respect to the outputs of M'_V is bounded.*

Proof. From [31][Theorem 3.6] and Ernst et al. [8], which state that the RMS error of a GPC approximation is proportional to o_{gpc}^{-p} , where p is a positive value that depends on the smoothness of the function being approximated.¹ \square

Corollary 1 (GPC Convergence). *As $o_{gpc} \rightarrow \infty$, RMS error of GPC approaches 0, that is, M_{GPC} can be an arbitrarily close approximation of M'_V .*

Lemma 2 (Perception Model Convergence). *Assume that for a particular environment distribution \mathcal{D}_E , the distribution of neural network outputs in any state is Gaussian. Then, the output distribution of the perception model M_{per} in any state approaches the real neural network output distribution at that state as $|G|, N_i$, and the degree of the perception model are increased.*

Proof Sketch. Increasing the density of the state tensor grid G increases the number of ground truth states used to train the perception model. Increasing N_i increases the accuracy of the neural network output distribution calculated at each grid point. Thus, after we increase the number and accuracy of the training data points, the accuracy of the perception model can be arbitrarily increased by increasing the degree of polynomial regression (increasing only the degree of polynomial regression leads to overfitting; increasing the amount of training data first is necessary.) \square

¹ For M'_V , the process of obtaining the neural network output sample using the perception model and the vehicle dynamics are usually smooth. However, the control system components may not be differentiable everywhere.

Theorem 2 (GAS Convergence). *Assume that for a particular environment distribution \mathcal{D}_E , the distribution of neural network outputs in any state is Gaussian. Then, the GAS model M_{GPC} converges in output distribution to the original vehicle model M_V .*

Proof Sketch. Since we can construct an arbitrarily accurate perception model (Lemma 2), we can use it to obtain accurate neural network output samples for any state through M'_V . The GPC model can be made an arbitrarily accurate approximation of M'_V (Corollary 1), and thus of M_V . \square

Practically, controlling the error of the perception model (or any approximation of a neural network) is an open problem [4,22]. While precise analytic calculation of the perception model error is often not tractable, we can empirically estimate the error after the approximation. After creating M'_V , M_{GPC} will be the optimal polynomial model of it for any o_{gpc} ([31][Equation 5.9]).

Finally, our assumption that neural network outputs have a Gaussian distribution impacts accuracy. We can use standard statistical tests (e.g., the Shapiro-Wilk test or the Anderson-Darling test) to check if the assumption is satisfied while gathering perception model training data. If the distribution is not approximately Gaussian, one can use a different base distribution (and orthogonal polynomial) that would better fit the data.

C Vehicle Models with Categorical State Variables

Some vehicle models have categorical state variables. For example, consider an autonomous plane which avoids a collision by following advisories from a Collision Avoidance System (CAS) such as [15]. CAS systems take into consideration the advisory given in the previous time step when giving the advisory for the current time step. The model for such a vehicle accepts the previous advisory as a state variable, and returns the current advisory as part of its updated state.

Unlike categorical variables, polynomial inputs and outputs are totally ordered. Therefore, we cannot use GPC for predicting categorical variables. Similarly, we cannot accept a categorical variable as an input to the GPC model. GAS solves this problem by splitting the GPC approximation problem and using a separate classifier for predicting categorical variables.

Consider a vehicle model M_V whose state includes a categorical variable X with the domain $\mathbb{D}_X = \{x_1, \dots, x_k\}$. GAS uses MEGPC to create a separate GPC approximation for each $x_i \in \mathbb{D}_X$. GAS chooses which of these approximation to use based on the input to the vehicle model. These GPC approximations calculate all output state variables except X .

For predicting the value of X in the output of M_V , GAS creates an ancillary classifier, which it trains as follows:

1. GAS picks a set of states G from the safe states \mathbb{D}_S^S , such that G is an evenly spaced tensor grid that includes the most extreme states within \mathbb{D}_S^S , and includes all categorical values in \mathbb{D}_X .

2. For each $g \in G$, GAS evaluates $M_V(g, E, R)$ for a large number of samples (≥ 350) of E and R . GAS isolates the value of X in the output and calculates the mode value.
3. GAS trains a classifier to predict the mode output X value for any $S \in \mathbb{D}_S^S$.

GAS returns the mode predicted by the classifier as the value of X in the output. This method can be generalized to multiple categorical variables, but the number of separate GPC approximations required can become impractical.

D Visual Distribution Comparisons at Final Time Step

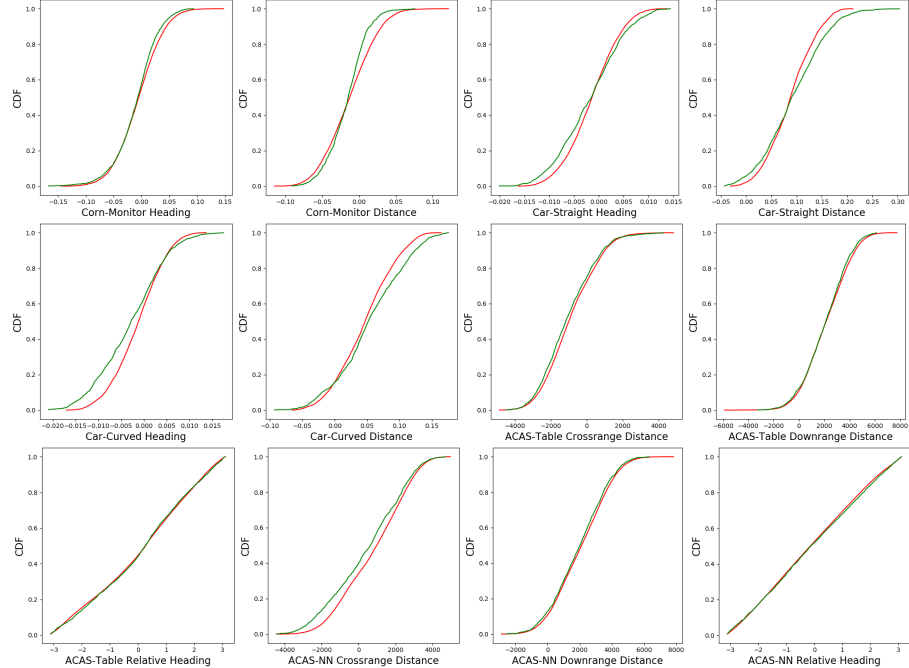


Fig. 10: Distribution comparison at final time step. Red: GAS, Green: MCS.

Figure 10 shows a visual comparison of the distributions of each state variable of each benchmark at the final (100^{th}) time step. The red plots show the CDF of the distribution obtained using GAS, while the green plots show the distribution obtained using MCS. The name of each benchmark and state variable is below the corresponding comparison. Visually, the MCS and GAS distributions closely resemble each other.

E How do Perception Model Parameters Affect GAS Accuracy?

Table 5: Effect of varying perception model parameters on maximum KS statistic (* denotes the value in the evaluation). C-M: Corn-Monitor, C-S: Car-Straight, t_{rel} : relative time.

G	C-M	C-S	t_{rel}	N_i	C-M	C-S	t_{rel}	degree	C-M	C-S	t_{rel}
7x7	0.201	0.126	0.40 \times	100	0.288	0.120	0.29 \times	3	0.096	0.115	1.00 \times
9x9	0.084	0.126	0.67 \times	350*	0.081	0.126	1.00 \times	4*	0.081	0.126	1.00 \times
11x11*	0.081	0.126	1.00 \times					5	0.192	0.176	1.00 \times

We varied the parameters of the perception model, specifically G , N_i , and the degree of polynomial regression, to measure their effect on accuracy. Table 5 shows how these parameters affect the maximum KS statistic for Corn-Monitor (C-M) and Car-Straight (C-S). Smaller grid sizes (Columns 1-4) and number of images per grid point (Columns 5-8) decrease the time required to create the perception model (t_{rel} is relative time usage), but greatly hinder accuracy. We limit grid size to 11x11 as accuracy improvement over a 9x9 grid is minimal. Similarly, increasing N_i beyond 350 gives diminishing returns. Using larger grids or N_i would unnecessarily increase the time required to create the perception model. A degree 4 polynomial regression model appears to provide the highest accuracy (Columns 9-12); further increasing degree reduces accuracy (due to overfitting).

In conclusion, perception model parameters can have a significant effect on end-to-end GAS results, and we must choose them carefully for optimal accuracy.

F Additional Sensitivity Analysis Plots

Below are additional sensitivity analysis plots for all benchmarks. Each subplot corresponds to one sensitivity index. In all plots, the X-Axis shows the number of MCS simulations, while the Y-Axis shows the value of the sensitivity index. The red plots correspond to the value analytically calculated by GAS, while the green plots correspond to the value empirically calculated using MCS. Below each subplot, the label $X \rightarrow Y$ indicates that the subplot is for the effect of the input variable X on the output variable Y after one time step. Raw0 and Raw1 correspond to the raw sample used by the perception model for the Corn-Monitor and Car benchmarks. In most cases, the MCS values reach those calculated by GAS after $10^6 - 10^7$ samples. In some cases where the sensitivity index is very close to 0 or 1, the MCS and GAS values still differ. This is likely due to the accuracy of GAS w.r.t. the abstracted vehicle model. However, as indicated by the Y-Axis, these differences are very small in the absolute sense.

